Journal of
Experimental
Botany
www.jxb.oxfordjournals.org

RESEARCH PAPER

Dynamics of leaf hydraulic conductance with water status: quantification and analysis of species differences under steady state

Christine Scoffoni*, Athena D. McKown, Michael Rawls and Lawren Sack

Department of Ecology and Evolutionary Biology, University of California, Los Angeles, 621 Charles E. Young Drive South, Los Angeles, CA 90095-1606, USA

* To whom correspondence should be addressed. E-mail: cscoffoni@ucla.edu

Abstract

Leaf hydraulic conductance (K_{leaf}) is a major determinant of photosynthetic rate in well-watered and drought-stressed plants. Previous work assessed the decline of K_{leaf} with decreasing leaf water potential (Ψ_{leaf}), most typically using rehydration kinetics methods, and found that species varied in the shape of their vulnerability curve, and that hydraulic vulnerability correlated with other leaf functional traits and with drought sensitivity. These findings were tested and extended, using a new steady-state evaporative flux method under high irradiance, and the function for the vulnerability curve of each species was determined individually using maximum likelihood for 10 species varying strongly in drought tolerance. Additionally, the ability of excised leaves to recover in K_{leaf} with rehydration was assessed, and a new theoretical framework was developed to estimate how rehydration of measured leaves may affect estimation of hydraulic parameters. As hypothesized, species differed in their vulnerability function. Drought-tolerant species showed shallow linear declines and more negative Ψ_{leaf} at 80% loss of K_{leaf} (P_{80}), whereas drought-sensitive species showed steeper, non-linear declines, and less negative P_{80}. Across species, the maximum K_{leaf} was independent of hydraulic vulnerability. Recovery of K_{leaf} after 1 h rehydration of leaves dehydrated below their turgor loss point occurred only for four of 10 species. Across species without recovery, a more negative P_{80} correlated with the ability to maintain K_{leaf} through both dehydration and rehydration. These findings indicate that resistance to K_{leaf} decline is important not only in maintaining open stomata during the onset of drought, but also in enabling sustained function during drought recovery.

Key words: Cavitation, dehydration, EFM, K_{leaf}, rehydration, refilling, safety margins, turgor loss point, vulnerability curves

Introduction

In dicotyledons, the leaf hydraulic conductance strongly constrains gas exchange and growth (Sack *et al.*, 2003; Sack and Holbrook, 2006). The resistance of open stomata to vapour diffusion out of the leaf is typically far greater than the hydraulic resistance to bulk flow of the liquid through the plant, and transpiration rates are thus dictated by this diffusion process, which in turn depends on the stomatal and boundary layer conductances and the difference in vapour pressure between the intercellular air spaces of the leaf and the atmosphere (Cowan, 1972; Sack and Tyree, 2005; Sack and Holbrook, 2006). However, the mainte-

nance of open stomata depends on the leaf being well hydrated; that is, having a high leaf water potential (Ψ_{leaf}), which, in turn, depends on the plant hydraulic conductance being sufficiently high. Because in dicotyledons, the leaf accounts for on average 30% of the plant hydraulic resistance (Sack *et al.*, 2003; Sack and Holbrook, 2006), the leaf hydraulic conductance (K_{leaf}=flow rate/water potential driving force, i.e. 1/leaf hydraulic resistance) is thus a critical variable. Water enters the petiole, moves through several vein orders of diminishing size, then exits into the bundle sheath and moves through or around cells before

evaporating into the intercellular airspace and being transpired from the stomata. The K_{leaf} declines with ψ_{leaf} during drought, due to losses of conductance resulting from cavitation and/or collapse of xylem conduits, and/or to decline in the permeability of extra-xylem tissues, and this response drives stomatal closure to prevent leaf desiccation (e.g. Salleo *et al.*, 2000; Brodribb and Holbrook, 2004a; Sack and Holbrook, 2006; Scoffoni *et al.*, 2008; Brodribb and Cochard, 2009; Brodribb *et al.*, 2010; Scoffoni *et al.*, 2011). Understanding species variation in hydraulic vulnerability is thus critical, and several techniques have been applied, especially the rehydration kinetics method (RKM; Supplementary Table S1 available at *JXB* online; Brodribb and Holbrook, 2003a). The aim of this study was to quantify this response using an independent, steady-state method, for species varying strongly in drought tolerance, and to determine the ability of dehydrated leaves to recover in K_{leaf} after rehydration.

Previous studies using the RKM found species to vary strongly in leaf hydraulic vulnerability, quantified as the Ψ_{leaf} at 50% loss of K_{leaf} (P_{50}; e.g. Hao *et al.*, 2008; Blackman *et al.*, 2009; Chen *et al.*, 2009; Johnson *et al.*, 2009a; Saha *et al.*, 2009). Additionally, species with a low P_{50} also had low osmotic potential at the turgor loss point (Blackman *et al.*, 2010), and could thus maintain stomata open as leaves dehydrate. Further, these studies tested the classic trade-off between hydraulic efficiency and safety, previously found for stems, and showed this to be absent in leaves: the maximum K_{leaf} for hydrated leaves (K_{max}) was independent of P_{50} (Sack and Holbrook, 2006; Blackman *et al.*, 2010).

Notably, the various methods for measuring K_{leaf} all have value but can raise potential concerns (Sack and Tyree, 2005). There was thus a need to test leaf hydraulic vulnerability with a method independent of the RKM. The typically used RKM measures K_{leaf} from water uptake into the mesophyll of a dehydrated leaf for a known time, and involves some uncertainty because uptake to leaf cells continues even after leaf collection for Ψ_{leaf} determination, though a recently modified version of the RKM ('dynamic RKM') has overcome this limitation (Brodribb and Cochard, 2009; Blackman and Brodribb, 2011; Brodribb, Blackman, and PrometheusWiki contributors, 2011). Additionally, in the RKM, water uptake into mesophyll cells might not always mimic the complete pathways of natural transpiration (Scoffoni *et al.*, 2008). Furthermore, the RKM may give low resolution of K_{leaf} declines in the well-hydrated range of the vulnerability curve if such leaves rehydrate completely during measurement. The evaporative flux method (EFM) has the advantage of allowing K_{leaf} measurement during steady-state transpiration and, further, using the EFM, leaves can be acclimated to high irradiance, which influences K_{leaf} for many species (Sack *et al.*, 2002; Nardini *et al.*, 2005; Tyree *et al.*, 2005; Cochard *et al.*, 2007; Sellin and Kupper, 2007; Scoffoni *et al.*, 2008; Sellin *et al.*, 2008). One previous study applied a variant of the EFM to generate vulnerability curves (the heat-flux method, 'Heat-FM'; Brodribb and Holbrook, 2006) which involved some

complexity. A heat gun was used on the leaf to drive a transiently high transpiration rate, after which the stomata closed, establishing a lower flow rate. The leaf was removed, and K_{leaf} was determined as the steady-state flow rate divided by the final Ψ_{leaf} (Ψ_{final}), and the vulnerability curve was determined as K_{leaf} plotted against Ψ_{final}. However, that method could not determine the lowest Ψ_{leaf} induced in the leaf during the high transpiration rates driven by the hot air (Ψ_{lowest}), which may have triggered the K_{leaf} decline. In this study, the EFM was modified to allow measurement of both Ψ_{lowest} and Ψ_{final}, such that K_{leaf} could be plotted against both.

A second aim of this study was to refine the statistical analysis of the K_{leaf} decline with dehydration for improved accuracy and mechanistic insight. Typically, studies have fitted the same function for all species, chosen for approximate fit to the data; polynomial (including linear), sigmoidal, and logistic functions have all been used (Supplementary Table S1 at *JXB* online). However, species may differ in the shape of their vulnerability curve, and choosing the appropriate function is important both for accuracy and also to allow interpretation of the underlying processes (Brodribb and Holbrook, 2006, 2007). Notably few studies have directly discussed the underlying basis for different shapes of vulnerability curves, probably due to the lack of an approach to select the appropriate function objectively, but the literature has pointed to several potential mechanisms for differently shaped curves (reviewed in Table 1). As a next step, a rigorous analysis is needed to resolve species differences in the shape of the function. Thus, for 10 diverse species, the maximum likelihood function was selected for each species. Drought-tolerant species were hypothesized to show shallower, linear declines, whereas drought-sensitive species were expected to show stronger initial K_{leaf} declines due to greater sensitivity in one or more components of the water transport system. Tests were made of the impact on estimated hydraulic vulnerability parameters of using different functions as in previous studies (Supplementary Table S1), and the degree to which it matters how vulnerability curves are plotted, namely whether unbinned data for K_{leaf} are plotted against Ψ_{lowest} or Ψ_{final}, or whether data are binned by Ψ_{leaf} intervals.

A third aim in this study was to quantify the recovery of K_{leaf} with rehydration, a related, essential process that has received little attention. One previous study found that excised and dehydrated sunflower leaves recovered rapidly in K_{leaf} when rehydrated with petioles under water (Trifilo *et al.*, 2003a). Species differences in this ability were tested for. Species with the greatest hydraulic vulnerability were hypothesized to show the greatest recovery, as they would derive most benefit. Further, all studies of vulnerability have involved leaf rehydration during measurement, but none has accounted for this in interpretation; tests were developed to determine how the measurements might be affected. The main benefit of a low hydraulic vulnerability has typically been framed as the ability to keep stomata open without dehydrating the mesophyll. It was hypothesized that a low hydraulic vulnerability would also confer

Table 1. Mechanisms that would theoretically influence the shape of the response of leaf hydraulic conductance (K_{leaf}) to dehydration (i.e. decreasing leaf water potential, Ψ_{leaf}) and thus the function that best fitted to the data. A linear decline implies no threshold Ψ_{leaf} before which K_{leaf} declines (i.e. K_{leaf} declines immediately as Ψ_{leaf} declines), and also a proportional decline of K_{leaf} with Ψ_{leaf}. A non-linear decline of K_{leaf} with Ψ_{leaf} can include a threshold Ψ_{leaf} before the decline begins and/or a disproportionate decline of K_{leaf} as Ψ_{leaf} declines. For these possibilities three types of mechanisms were included—those relating to air seeding causing cavitation in the xylem conduits (and analogous effects would occur given collapse of xylem conduit walls), those arising from venation architecture, and those arising in the pathways outside the xylem. References are provided to studies of these potential mechanisms *per se* and/or on their influence on the shape of stem or leaf vulnerability curves.

Shape of K_{leaf} decline	Air seeding	Venation architecture	Pathways outside the xylem
Linear decline:			
No threshold before decline	If air seeding begins at high Ψ_{leaf} because of large pit membrane pore size (Neufeld et al., 1992; Pammenter and Vander Willigen, 1998)		If a loss of membrane permeability (e.g. due to aquaporin activity or loss of cell turgor) begins immediately as Ψ_{leaf} declines (Brodribb and Holbrook, 2006)
Proportional decline of K_{leaf} with declining Ψ_{leaf}	If conduits of different sizes all have a wide range in maximum pit membrane pore size such that cavitation occurs equally across conduit sizes (Pammenter and Vander Willigen, 1998; Choat et al., 2005)	If higher major vein length/area (=vein density) confers hydraulic redundancy, such that first embolisms of the vein xylem conduits do not cause a dramatic decline (Scoffoni et al., 2011)	If membrane permeability declines linearly as the average cell tugor declines with Ψ_{leaf} (Kubiske and Abrams, 1990; Brodribb and Holbrook, 2006). If the K_{leaf} declines due to loss of water-filled pathways through cell walls (Pieruschka et al., 2010)
Non-linear decline (logistic, sigmoidal, exponential):			
Threshold before decline	If a threshold for air seeding determined by the largest pit membrane pore size leads to a retention of K_{leaf} until a Ψ_{leaf} threshold (Neufeld et al., 1992; Pammenter and Vander Willigen, 1998; Domec et al., 2006)		If there is a threshold Ψ_{leaf} below which aquaporins are deactivated and membrane permability declines (North and Nobel, 2000; Miyazawa et al., 2008). If the K_{leaf} is insensitive to turgor or turgor is maintained by osmotic adjustment until a cavitation threshold is reached (Brodribb and Holbrook, 2006)
Disproportionate decline of K_{leaf} with declining Ψ_{leaf}	If larger conduits conferring the bulk of the vein xylem conductivity have larger pit membrane pores or greater pore numbers, and cavitate first, followed by smaller conduits that have decreasing impact on K_{leaf} (Neufeld et al., 1992; Pammenter and Vander Willigen, 1998; Tyree and Zimmermann, 2002)	If leaves with lower major vein density suffer strong decline in K_{leaf} with first embolism of xylem conduits in the low-order veins (Scoffoni et al., 2011)	If strong declines due to aquaporin deactivation occur at high Ψ_{leaf} (Johansson et al., 1998; Kim and Steudle, 2007; Scoffoni et al., 2008). If a greater loss of turgor in cells with relatively weak solute potential (e.g. bundle sheath cells) during leaf dehydration lead to especially rapid decline in K_{leaf} (Nonami and Schulze, 1989; Koroleva et al., 1997)

the ability to maintain K_{leaf} through both dehydration and rehydration.

Materials and methods

Plant material

This study was conducted alongside a study of the importance of venation architecture and leaf size in determining species variation in hydraulic vulnerability (Scoffoni et al., 2011). Ten species were selected across nine families and spanning a wide range of drought sensitivity; five species were native to dry habitats (mainly California chaparral) and five species to moist habitats (Table 2). Study species included mature trees and shrubs in and around the

campus of University of California, Los Angeles and Will Rogers State Park, Los Angeles, California, and sunflower *Helianthus annuus* var. Sunspot grown from seeds (Botanical Interests; Broomfield, Colorado, USA) in 3.6 l pots in a greenhouse (average minimum, mean, and maximum values for temperature. 21.1, 23.2, and 26.0 °C; for humidity, 44, 51, and 59%). Sunflowers were irrigated every 2 d, with 200–250 ppm of 20:20:20 N:P:K; the irradiance measured at mid-day on a sunny day was up to 550 μmol photon m^{-2} s^{-1}, and on average 300 μmol photon m^{-2} s^{-1} (LI-250 light meter; LI-COR Biosciences, Lincoln, NE, USA).

Experiments were conducted in May–September 2008. On the day prior to measurements, for 3–10 plants per species, exposed branches with mature, healthy leaves were collected into plastic bags with moist paper towel; for sunflowers, whole shoots were collected. Each shoot was re-cut by at least two nodes in the

Table 2. Study species, family, native range, and mean values ±SE for pressure–volume curve parameters and leaf hydraulic vulnerability parameters, i.e. leaf hydraulic conductance at full hydration (K_{max}), leaf water potential at 50% and 80% decline of leaf hydraulic conductance (P_{50} and P_{80}), calculated from the maximum likelihood function for the 'Ψ_{lowest} unbinned' plot, and results of t-tests on species' means (for hydraulics parameters) or of analyses of variance for the difference between moist and dry area species, and among species nested within those categories (for pressure–volume parameters). Data are from Scoffoni et al. (2011).

Species	Family	Native range[a]	K_{max} (mmol m^{-2} s^{-1} MPa^{-1})	P_{50} (–MPa)	P_{80} (–MPa)	Turgor loss point (–MPa)	Osmotic potential (–MPa)	Modulus of elasticity (MPa)	Saturated water content (g g^{-1})
Dry habitat species									
Cercocarpus betuloides	Rosaceae	California. Mexico	4.36	2.76	5.25	2.59±0.03	1.64±0.04	10.1±0.701	0.79±0.02
Comarostaphylis diversifolia	Ericaceae	California. Mexico	2.96	2.85	4.56	3.45±0.34	2.51±0.34	17.3±2.23	0.70±0.01
Hedera canariensis	Araliacaeae	Canary Islands	5.73	0.64	1.18	1.98±0.09	1.49±0.07	17.9±1.28	2.81±0.09
Heteromeles arbutifolia	Rosaceae	California. Mexico	20.7	2.57	4.12	2.53±0.10	2.08±0.10	16.4±0.486	1.38±0.07
Quercus agrifolia	Fagaceae	California. Mexico	3.96	2.40	3.83	3.00±0.12	2.31±0.12	12.8±0.787	0.93±0.01
Moist habitat species									
Camellia sasanqua	Theaceae	Japan	5.99	1.78	2.84	2.12±0.18	1.61±0.04	7.98±1.11	1.74±0.03
Helianthus annuus	Asteraceae	Across N. America	6.45	0.83	1.16	1.09±0.12	0.875±0.10	13.3±1.31	11.2±0.79
Lantana camara	Verbenaceae	Pantropical	11.4	0.80	1.41	1.37±0.04	1.10±0.04	9.14±0.525	2.73±0.15
Magnolia grandiflora	Magnoliaceae	Southern USA	5.24	0.42	2.06	2.06±0.05	1.43±0.34	5.49±0.792	1.50±0.07
Platanus racemosa	Platanaceae	California, Mexico	34.1	0.09	0.35	2.03±0.06	1.54±0.12	4.85±0.331	1.34±0.03
Average ±SE	Dry habitat species		7.55±3.32	2.24±0.41	3.79±0.69	2.71±0.14	2.01±0.19	14.9±1.49	1.32 ±0.04
	Moist habitat species		12.6±5.48	0.78±0.28	1.56±0.42	1.74±0.09	1.31±0.14	8.16±1.51	3.71 ±0.21
ANOVA or t-test	Dry/moist species		NS	*	*	***	***	***	***
						***	***	***	***

[a] *Croat (1978)*; *Kitamura and Murata (1979)*; eFloras (2008).
NS, P >0.05; *P <0.025;***P <0.001.

laboratory under ultrapure water (MilliPore, 0.22 μm Thornton 200CR, Molshem, France) and rehydrated overnight at laboratory temperature (20–25 °C), covered with dark plastic bags.

Measuring the dehydration response of K$_{leaf}$ with the evaporative flux method

Using the EFM, K_{leaf} is determined as the ratio of steady-state transpirational flow rate (E, mmol m^{-2} s^{-1}) to the water potential driving force ($\Delta\Psi_{leaf}$, MPa; Sack *et al.*, 2002). Notably, in this system, the overall driving force for flow through the whole leaf is the water potential gradient between the outside air and the water entering the petiole, but the important component of that driving force is the vapour pressure gradient between the outside air and leaf air spaces; this vapour pressure driving force, and stomatal conductance, determine the transpiration rate (see Introduction). However, for the liquid phase part of flow (i.e. the hydraulic system), the driving force at steady state is the water potential gradient between the leaf mesophyll where water evaporates (estimated as the Ψ_{leaf} measured at the end of the measurement,

i.e. the Ψ_{final}) and the water entering the petiole at atmospheric pressure (i.e. 0 MPa relative pressure).

In this study, the focus was on the dehydration response of the whole-leaf hydraulic system, including the petiole. The leaf was cut from the shoot with a fresh razor blade under ultrapure water that was used as flow solution (0.22 μm Thornton 200 CR; MilliPore), degassed for at least 8 h with a vacuum pump (Gast, Benton Harbor, MI, USA), and refiltered (0.2 μm; Syringe filter, Cole-Parmer, Vernon Hills, IL.USA). The petiole was then rapidly connected to silicon tubing (Cole-Parmer) under ultrapure water to prevent air entering the system. The tubing connected the leaf to a cylinder on a balance (models XS205 and AB265, ±10 μg sensitivity; Mettler Toledo, Columbus, OH, USA) that logged data every 30 s to a computer for the calculation of flow rate through the leaf (E). Leaves were held adaxial surface upwards in wooden frames strung with fishing line above a large box fan (Lakewood Engineering & Manufacturing Company, Chicago, IL, USA). Leaves were illuminated with >1000 mmol m^{-2} s^{-1} photosynthetically active radiation at the leaf surface by floodlights (model 73828 1000 W, 'UV filter'; Sears, Roebuck, Hoffman Estates, IL, USA) suspended above a Pyrex container (Corning Incorporated,

Corning, NY, USA) filled with water to absorb the heat of the lamp. Leaf temperature was determined using a thermocouple (Cole-Parmer) and maintained between 23 °C and 28 °C.

Leaves were allowed to transpire on the apparatus for at least 30 min and until the flow rate stabilized, with no upward or downward trend, and with a coefficient of variation <5% for at least five measurements made at 30 s flow intervals. When the flow rate was very low (<8 μg s^{-1}), stability was determined with the same criterion, but using the running averages of the last five 30 s intervals. Previous studies found these criteria to be sufficient for stabilization of E, Ψ_{leaf}, and K_{leaf}; tests with longer measurement periods after stable flow was established showed no relationship of K_{leaf} to measurement time for seven species of a wide range of leaf capacitance (Scoffoni *et al.*, 2008; Pasquet-Kok *et al.*, 2010). The minimum 30 min flow period was chosen to ensure that leaves had sufficient time to acclimate to high irradiance, which has been found to enhance K_{leaf} by up to 8-fold depending on species, apparently due to the expression and/or activation of aquaporins (Sack *et al.*, 2002; Nardini *et al.*, 2005; Tyree *et al.*, 2005; Cochard *et al.*, 2007; Scoffoni *et al.*, 2008; Voicu *et al.*, 2008). Measurements were discarded if the flow suddenly changed, due either to apparent leakage from the seal or to blockage in the system by particles or air bubbles. Following the stabilization of the flow rate, leaf temperature was recorded with a thermocouple and the final five flow rate measurements were averaged. The leaf was quickly removed from the tubing, the petiole was dabbed dry, and the leaf was placed into a sealable bag (Whirl-Pak; Nasco, Fort Atkinson, WI, USA), which had been previously exhaled in, to halt transpiration. Following at least 30 min equilibration, the final leaf water potential (Ψ_{final}) was measured with a pressure chamber (Plant Moisture Stress, Model 1000, Albany, OR, USA). K_{leaf} was calculated as $E/-\Delta\Psi_{leaf}$ (where $\Delta\Psi_{leaf}=\Psi_{final}-0$ MPa) and further normalized by leaf area measured with a LI-COR 3100 leaf area meter. To correct for changes in K_{leaf} induced by the temperature dependence of water viscosity, K_{leaf} values were standardized to 25 °C (Weast, 1974; Yang and Tyree, 1993; Sack *et al.*, 2002).

To determine the stomatal conductance of leaves measured with the EFM, the final E was divided by the mole fraction vapour pressure deficit (VPD), derived from temperature and relative humidity (RH) measurements in the lab from a weather station that logged measurements every 5 min (HOBO Micro Station with Smart Sensors; Onset, Bourne, MA, USA), where mole fraction VPD=[1–(RH×VP_{sat})]/101.3 kPa, and VP_{sat} is the saturation vapour pressure determined using the Arden Buck equation (Buck, 1981).

The EFM was modified to allow determination of K_{leaf} for dehydrated leaves. Shoots were cut into segments with at least three leaves under ultrapure water and then dehydrated with a fan for different periods of time to a range of Ψ_{leaf} values. The bench drying of shoots to achieve a leaf vulnerability curve has been used in studies using the RKM (e.g. Brodribb and Holbrook, 2003*a*; Blackman *et al.*, 2009), and previous studies found similar vulnerability curves when constructed from bench-drying shoots as from leaves on plants progressively droughted (Brodribb and Holbrook, 2004*a*; Blackman *et al.*, 2009; Pasquet-Kok *et al.*, 2010). In the present study, shoots were allowed to equilibrate for at least 30 min before two leaves were excised and measured for initial Ψ_{leaf} (Ψ_o) using a pressure chamber. If the difference in the Ψ_{leaf} of those two leaves was >0.1 MPa, the shoot was discarded; for very dehydrated shoots, this range was extended to 0.3 MPa. The third leaf (typically the middle leaf) was used to determine K_{leaf} with the EFM. When dehydrated leaves are measured with the EFM, the stomata open (see Results); before steady-state flow is achieved, the leaf may rehydrate such that Ψ_{final} is less negative than Ψ_o, or, alternatively, the leaf may further dehydrate such that Ψ_{final} is more negative than Ψ_o. For each species, at least six K_{leaf} values were obtained for each 0.5 MPa interval from full hydration to strong dehydration. Outlier tests were conducted for each 0.5 MPa interval (Dixon test; Sokal and Rohlf, 1995); 0–4 outliers

were removed over the whole curve for given species (representing 0–8% of the 26–74 data points per curve).

To test the importance of the method for constructing vulnerability curves, these were determined in three ways previously applied (Supplementary Table S1 at *JXB* online). First, K_{leaf} was plotted against whichever was lowest, Ψ_o or Ψ_{final} (='Ψ_{lowest}'); that is, the Ψ_{leaf} associated with the strongest dehydration experienced during the experiment, and each leaf was considered as a data point ('unbinned Ψ_{lowest}'). Additionally, K_{leaf} was plotted against Ψ_{lowest} with data averaged in 0.5 MPa bins ('binned Ψ_{lowest}'), with the exception of *H. annuus* averaged in 0.2 MPa bins because of its distinctively narrower K_{leaf} response, with negligible values below –1.5 MPa. Finally, K_{leaf} was plotted against Ψ_{final} rather than Ψ_{lowest} ('Ψ_{final}'), with each leaf considered as a data point. Determination of these alternative versions of the vulnerability curve also allowed interpretation of the recovery of K_{leaf} during the measurement (see section below).

In the above-described methods, as in previous studies of K_{leaf}, the pressure chamber balance pressure was taken as Ψ_{leaf}. In actuality, the balance pressure for an equilibrated leaf gives the xylem pressure potential (P_x), and $-P_x$ is less negative than the bulk Ψ_{leaf} by the amount of the vein xylem solute potential (π_x; Tyree and Zimmermann, 2002). Notably, previous studies on a range of species have measured π_x values of approximately –0.05 MPa, a difference that would not affect the present findings significantly (Boyer, 1967). Tests were carried out to verify such low π_x for *C. sasanqua*, *H. arbutifolia*, and *L. camara*. Shoots of four leaves were rehydrated overnight and dehydrated to a range of Ψ_{leaf} (–0.04 MPa to –1.5 MPa). Two leaves were excised for initial Ψ_{leaf} measurement, a third was bagged for determination of initial π_x, and the fourth was placed in the EFM apparatus until a steady-state flow rate was achieved. Leaf vein π_x was determined using vapour pressure osmometry (Vapro 5520, Wescor Inc., Logan, UT, USA). The leaf margin was excised to open the tips of the midrib and second-order veins, and the leaf was pressurized in the pressure chamber and xylem sap exuded from the petiole was collected onto a filter paper, while moist paper towels surrounded the chamber and petiole to minimize evaporation. The filter paper was transported to the osmometer in a weighing bottle filled with moist paper towel. All π_x values were less negative than the least negative measurable value with this instrument, –0.05 MPa, and thus indistinguishable from pure water in the instrument, indicating that the present findings would not be significantly impacted by π_x.

Model testing and estimation of parameters for the decline of K_{leaf} with dehydration

Maximum likelihood was used to select the function for each species' K_{leaf} vulnerability response (Burnham and Anderson, 2002), using the *optim* function in R 2.9.2 (http://www.r-project.org; Burnham and Anderson, 2004; Sack *et al.*, 2006; the scripts are available on request). A linear function ($K_{leaf}=a\Psi_{leaf}+y_o$), was tested, in addition to sigmoidal ($K_{leaf} = \frac{a}{1+e^{-\left(\frac{\Psi_{leaf}-x_0}{b}\right)}}$) and logistic functions ($K_{leaf} = \frac{a}{1+\left(\frac{\Psi_{leaf}}{x_0}\right)^b}$), as used previously in the literature on leaf vulnerability (Supplementary Table S1 at *JXB* online), and an exponential function ($K_{leaf} = y_0 + ae^{-b\Psi_{leaf}}$), as previously used for whole-plant vulnerability (Iovi *et al.*, 2009). The maximum likelihood parameters were determined by the Simulated Annealing procedure for global optimization, followed by the Nelder–Mead simplex procedure for local optimization; standard errors for parameters were generated from the Hessian matrix. For each data set, functions were compared using the Akaike Information Criterion (AIC), corrected for low n. The function with the lowest AIC value was chosen as the best fit function for that data set, with differences >2 considered as meaningful (Burnham and Anderson, 2002, 2004).

To compare species in their hydraulic parameters, and to determine correlations between hydraulic parameters and other leaf traits, values for the maximum K_{leaf} at full hydration (K_{max}) and the Ψ_{leaf} at which K_{leaf} had declined by 50% and 80% (P_{50} and P_{80}) were determined from the vulnerability curves. For these parameters, each species' maximum likelihood function was used [i.e. that with lowest AIC and highest r^2 determined from the unbinned data plots ('unbinned Ψ_{lowest}' and 'Ψ_{final}')]. The steepness of the vulnerability curve was also determined, as the first derivative of the maximum likelihood function at $\Psi_{leaf}= -0.5$ MPa, where the steepest declines were observed. As an additional method for determining K_{max}, the average K_{leaf} for points above -0.5 MPa was calculated for each species; this was the method used in most previous leaf hydraulics studies that measured only K_{leaf} for hydrated leaves, and not its vulnerability to dehydration (e.g. Sack *et al.*, 2002; Brodribb and Holbrook, 2003*b*; Nardini *et al.*, 2005).

To determine the degree to which the choice of function and data set matters, tests were made of the sensitivity of vulnerability curve parameters (K_{max}, P_{50}, and P_{80}) to the choice of function, and, for each function, of plotting K_{leaf} against 'unbinned Ψ_{lowest}', 'binned Ψ_{lowest}', or 'Ψ_{final}'.

Hydraulic safety margins were calculated as the difference between the Ψ_{leaf} at which the leaves of a given species lose turgor (π_{TLP}; data from Scoffoni *et al.*, 2011) and those at which hydraulic function was substantially lost (P_{50} or P_{80}). Positive numbers indicate a safety margin, whereas negative numbers indicate a loss of hydraulic function even above the turgor loss point.

Testing the recovery of leaf hydraulic conductance after dehydration

Experiments were performed to test the recovery of K_{leaf} for leaves rehydrated after dehydration (method after Trifilo *et al.*, 2003*a*). For the 10 species, shoots were dehydrated with a fan to a known Ψ_{leaf} below their respective turgor loss points (determined as described in the following section). Leaves from each shoot were excised in air using a fresh razor blade and measured for Ψ_{leaf} ($\Psi_{dehydration}$), and other leaves were excised under ultrapure water, and rehydrated for 1 h with their petioles under water in a beaker, covered with a dark plastic bag. Following rehydration, leaves were equilibrated in a plastic bag for at least 10 min and either had their petioles cut in air and were measured for Ψ_{leaf} ($\Psi_{rehydration}$), or had their petioles re-cut under ultrapure water and were immediately connected to the EFM to determine K_{leaf} ($n= 4$–12 per species). The percentage recovery of K_{leaf} was determined as the K_{leaf} after rehydration divided by the K_{leaf} at $\Psi_{dehydration}$, which was estimated from the species' maximum likelihood vulnerability curve $\times100\%$. The recovery was considered significant if the K_{leaf} after 1 h rehydration was greater than the K_{leaf} at $\Psi_{dehydration}$ (*t*-test; Minitab Release 15). The recovery was determined as complete if K_{leaf} after 1 h rehydration was not significantly lower than the K_{leaf} at $\Psi_{rehydration}$ which was estimated from the species' maximum likelihood vulnerability curve.

Testing for the recovery of leaf hydraulic conductance during EFM measurement

As in other methods for determining leaf hydraulic vulnerability (i.e. RKM and Heat-FM; see Introduction), the EFM partially rehydrates the dehydrated leaf, as the petiole is connected to water at atmospheric pressure. Two analyses were developed to test for the potential recovery of K_{leaf} during the EFM measurement. The first analysis was a test of residual variation. If K_{leaf} recovered completely during the EFM measurement, one would expect no influence of the dehydration treatment prior to measurement on the final K_{leaf} value; rather, the measured K_{leaf} would simply relate to Ψ_{final} (i.e. the leaf water potential during the final steady-state flow). Thus, for each species, from the maximum likelihood vulnerability curve for the 'Ψ_{final}' plot, the residuals of K_{leaf} against Ψ_{final} were calculated. These residuals represented the variation in K_{leaf} unrelated to Ψ_{final}. A test was made for correlation of these residuals with Ψ_{lowest} values (Minitab Release 15). If the residual K_{leaf} variation was negatively correlated with Ψ_{lowest}, there was a persistent impact of Ψ_{lowest} on K_{leaf}, independently of Ψ_{final}. In other words, the effect of the dehydration treatment persisted even at the end of the EFM measurement, and, thus, the K_{leaf} had not recovered completely during the measurement. The second analysis was the calculation of an index of the recoverability of K_{leaf} during the EFM. For each species, a sample of the vulnerability data was selected that was analogous to the 1 h rehydration experiment (see previous section). Data were selected for leaves that had been dehydrated to a Ψ_{leaf} below the turgor loss point but that had rehydrated during the EFM measurement to Ψ_{leaf} values similar to those for leaves measured by the EFM after the 1 h rehydration experiment ($n=4$–7 for each species). The percentage recovery of K_{leaf} during EFM was determined as the average measured K_{leaf} for this leaf sample divided by the K_{leaf} at $\Psi_{dehydration}$, which was estimated from the species' maximum likelihood vulnerability curve $\times100\%$. The significance of the recovery of K_{leaf} was tested as for leaves in the 1 h rehydration experiment.

Given that some species showed a partial recovery of K_{leaf} with rehydration during the EFM (see Results), a theoretical consideration was made of how K_{leaf} recovery during measurement should influence the calculation of vulnerability parameters. Based on the diversity of tissues in the leaf hydraulic pathway, the vulnerability of K_{leaf} is expected to involve several components, some of which might be recoverable on a short time scale, while others might be reversible after a longer time scale under low tension (cf. Brodribb and Holbrook, 2006; Scoffoni *et al.*, 2008). The most appropriate vulnerability plot would depend on the degree to which leaves are recoverable in the short term (Fig. 1). Bounding cases were considered in which (a) leaves were non-recoverable in K_{leaf} during the measurement; (b) leaves were totally recoverable; and (c) leaves were partially recoverable. In case (a) in which K_{leaf} is non-recoverable, an accurate vulnerability curve would be obtained by plotting K_{leaf} against Ψ_{lowest}, as only the minimum Ψ_{leaf} during the whole experiment is important for influencing K_{leaf}. In case (a), plotting K_{leaf} against Ψ_{final} would overestimate the leaf's vulnerability. In contrast, in case (b) in which K_{leaf} recovers completely during measurement, an accurate vulnerability curve would be determined by plotting K_{leaf} against Ψ_{final}, because only the Ψ_{leaf} during steady state at the end of the measurement is important for influencing K_{leaf}. In case (b), plotting K_{leaf} against Ψ_{lowest} would underestimate the leaf's vulnerability. Finally, in case (c), in which K_{leaf} is partially recoverable, the accurate vulnerability curve would be intermediate between the plots of K_{leaf} against Ψ_{final} and against Ψ_{lowest}. Additional scenarios were not considered, for example if leaves recover in K_{leaf} differently depending on their degree of dehydration; notably, such scenarios should fall within the bounding cases considered. Tests were conducted to determine whether the estimation of vulnerability parameters K_{max}, P_{50}, and P_{80} was improved by using for each species the plot appropriate to its K_{leaf} recovery. Thus, for the species that showed no K_{leaf} recovery during EFM measurement, parameters were re-calculated from the maximum likelihood function for the 'Ψ_{lowest} unbinned' plot and, for the species with partial recovery, parameters were averaged from those determined from the 'Ψ_{final}' and 'Ψ_{lowest} unbinned' plots. These re-calculated parameters were compared with those determined using the 'Ψ_{lowest} unbinned' for all species, as has been the most typical procedure in previous studies (Supplementary Table S1 at *JXB* online).

Statistical analysis of differences among species and trait correlations across species

Trait differences between moist and dry habitat species were tested using analyses of variance (ANOVAs) with species nested within habitat type, or by using *t*-tests on species means (Table 1; Minitab
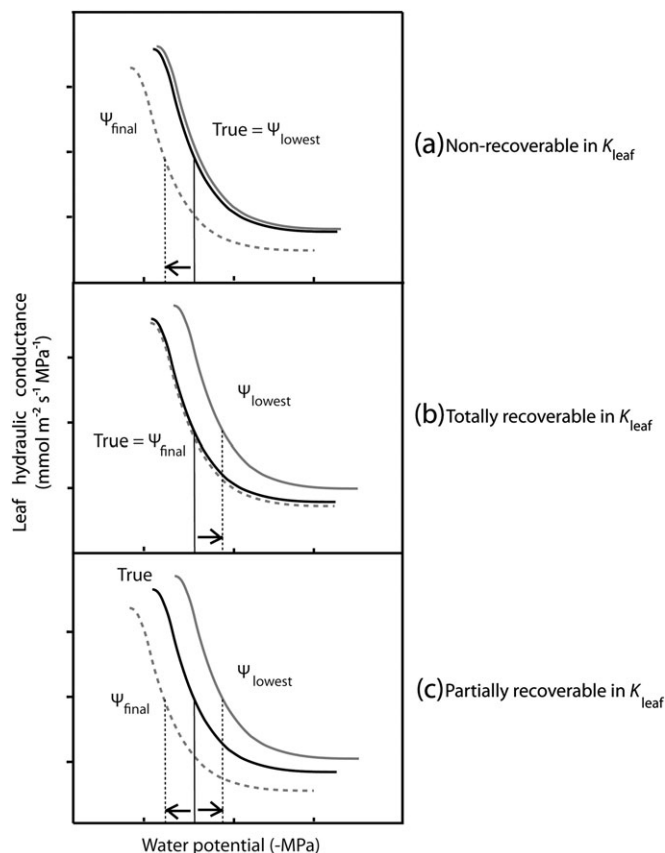
Fig. 1. A theoretical framework for the construction of vulnerability curves according to the degree that leaves recover in leaf hydraulic conductance (K_{leaf}) with rehydration. The black line is the 'true' vulnerability curve, the grey line is the vulnerability curve plotting K_{leaf} against 'Ψ_{lowest}', and the grey dotted line is the vulnerability curve plotting K_{leaf} against 'Ψ_{final}'. Bounding cases were considered: (a) leaves were non-recoverable in their K_{leaf} during the measurement; (b) leaves were totally recoverable in their K_{leaf}; and (c) leaves were partially recoverable in their K_{leaf} (see the Materials and methods).

Release 15). All data were log-transformed to improve normality and heteroscedasticity (Sokal and Rohlf, 1995). Correlations among traits were considered significant only if P <0.05 for both Spearman and Pearson coefficients (r_s and r_p, respectively); when relationships were non-linear, correlations for log-transformed data were determined. Standard major axes were fitted when determining slopes of relationships between traits, to account for error in both x and y variables (using SMATR; Sokal and Rohlf, 1995; Warton *et al.*, 2006).

Results

Vulnerability curves: species differences in the response of K_{leaf} to dehydration

The EFM was effective for determining vulnerability curves for leaves dehydrated from near full turgor to beyond the turgor loss point (Fig. 2). Leaves that had been previously dehydrated opened their stomata and established steady-state transpiration during the EFM measurement, as indicated by even the lowest transpiration rates observed
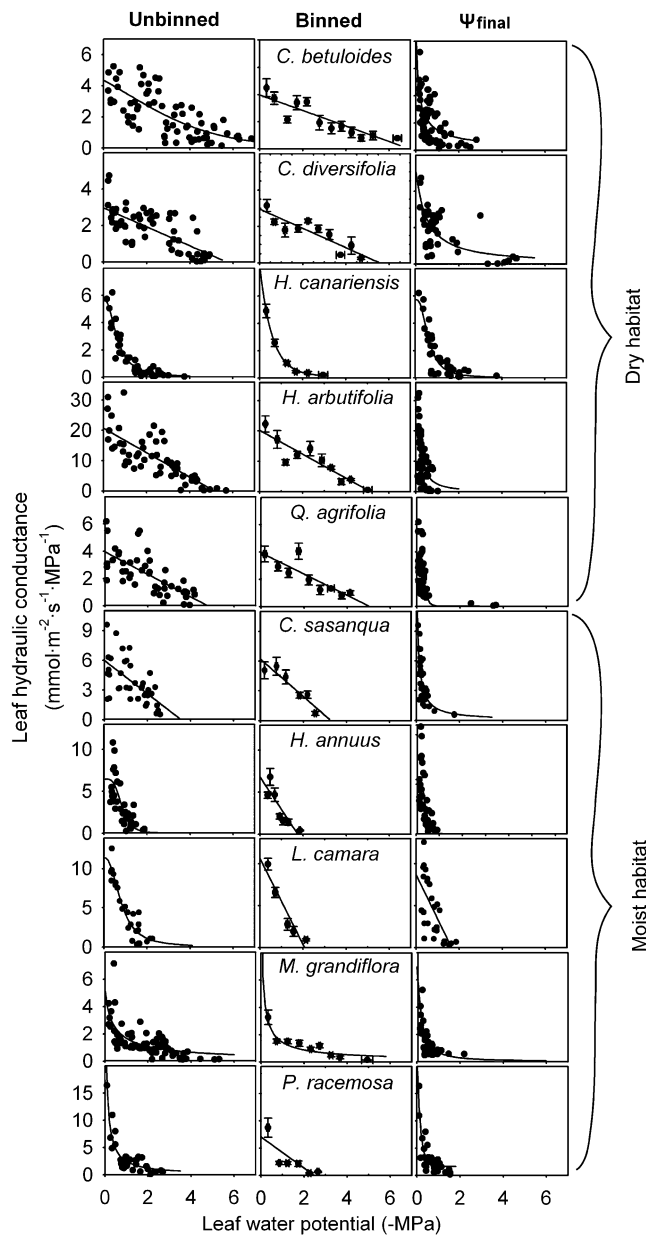

Fig. 2. Vulnerability curves for leaf hydraulic conductance (K_{leaf}) for 10 species varying widely in drought tolerance, determined using the evaporative flux method using three different plots ('Ψ_{lowest} unbinned', 'Ψ_{lowest} binned', and 'Ψ_{final}'). For the 'Ψ_{lowest} unbinned' and 'Ψ_{final}' panels, each point represents a different leaf measured. Standard errors are represented for each bin point in the 'Ψ_{lowest} binned' plot. The lines plotted are the maximum likelihood functions using each plot for each species (Supplementary Table S3 at JXB online).

representing stomatal conductance values 2.2- to 7.3-fold higher than cuticular conductance for these species (Supplementary Table S2 at *JXB* online).

Species differed significantly in the shape of the leaf hydraulic vulnerability curves. For four species the linear function was selected by maximum likelihood for K_{leaf} plotted against 'Ψ_{lowest} unbinned', and for six species a non-linear function was selected (Fig. 2; Supplementary Table S3 at *JXB* online). The logistic function was selected

for five species and the sigmoidal for *C. betuloides*. Species from dry habitats had a greater tendency to show a linear decline in K_{leaf} as one of their selected functions, that is, within an AIC of 2 of the maximum likelihood function (4/5 species versus 1/5 for moist habitats; $P=0.018$; proportion test). The slope of the vulnerability curve at $\Psi_{leaf}= -0.5$ MPa varied from -10 mmol m^{-2} s^{-1} MPa^{-2} to -0.5 mmol m^{-2} s^{-1} MPa^{-2}, and drought-sensitive species had on average 3-fold steeper slopes than drought-tolerant species (-6.5 mmol m^{-2} s^{-1} MPa^{-2} versus -1.6 mmol m^{-2} s^{-1} MPa^{-2}, respectively; *t*-test; $P=0.009, n=5$).

Vulnerability curves: sensitivity of derived parameters to the choice of function and plot

The use of maximum likelihood to select the vulnerability function for each species based on plots of K_{leaf} against 'Ψ_{lowest} unbinned' was considered to be the most appropriate practice, and was the one used for interpretation and comparison among species. However, because many previous studies have applied a single function and plot to all species' data, the sensitivity of the derived vulnerability parameters to the choice of function and plot and whether such choices affected the resolution of species ranking in vulnerability was tested. Notably, the functions selected by maximum likelihood with AIC values within 2 of the minimum depended on the choice of plot, and multiple functions were often selected for given species (Fig. 2, Supplementary Table S3 at *JXB* online). Thus, when using the 'Ψ_{lowest} binned' plot, the linear function was selected for 8/10 species, the logistic for two, and the exponential for one species. In contrast, when using the 'Ψ_{lowest} unbinned' plot, the logistic function was selected for eight species, the sigmoidal for six, the linear for five, and the exponential for four. When using the 'Ψ_{final}' plot, the logistic was selected for nine species, the exponential for eight, the sigmoidal for five, and the linear for two. The best fit function selected using the 'Ψ_{lowest} unbinned' plot was one of those selected when using the 'Ψ_{lowest} binned' data set for 5/10 species, and when using the 'Ψ_{final}' plot for only 3/10 species.

The estimation of vulnerability parameters K_{max}, P_{50}, and P_{80}, was sensitive to the function and the plot used, but typically the values determined in different ways were correlated across species (Fig. 2, data in Supplementary Table S4 at *JXB* online). When using the 'Ψ_{lowest} unbinned' plot, the K_{max}, P_{50}, and P_{80} values generated by the four different functions, averaged across species, varied by 12–27%, 0.21–0.76 MPa, and 0.12–0.74 MPa, respectively, and correlated across species in 15/18 comparisons ($r_p=0.81$–0.99; $P <0.05$). The use of the three plots produced K_{max} values from the four given functions that varied on average by 3–40%, and correlated across species in 11/12 comparisons ($r_p=0.64$–0.99; $P <0.05$; Fig. 2). Notably, for a species such as *Platanus*, with a steep initial hydraulic decline, determining K_{max} from a 'Ψ_{lowest} unbinned' plot was critical to resolve its high K_{max}. For P_{50} and P_{80}, the use of the 'Ψ_{lowest} unbinned' and 'Ψ_{lowest} binned' plots produced values for given functions that differed on average by 0.08–0.6 MPa, and correlated across species in 7/8 comparisons ($r_p=0.56$–0.99; $P <0.05$). In contrast, the use of the 'Ψ_{final}' plot produced P_{50} and P_{80} values 0.8–2 MPa less negative than when using the other plots (Fig. 2; paired *t*-test; $P <0.05$), and values were not correlated across species ($r_p= -0.40$ to 0.48; $P=0.11$–0.81). The values of K_{max} determined using the function selected using the 'Ψ_{lowest} unbinned' or 'Ψ_{lowest} binned' plots did not differ on average across species from those determined by taking the mean of K_{leaf} values at Ψ_{leaf} of 0 to -0.5 MPa (data in Supplementray Table S5 at *JXB* online; $P=0.10$–0.15; paired *t*-test). However, K_{max} determined using the 'Ψ_{final}' plot was on average 44% higher than K_{max} determined by taking the mean of K_{leaf} values at Ψ_{leaf} of 0 to -0.5 MPa ($P=0.02$), but again the species' values with the two methods were correlated ($r_p=0.74$; $P <0.01$).

Species variation in maximum K$_{leaf}$ and vulnerability, and lack of an efficiency–safety trade-off

Species were compared in the parameters determined from their maximum likelihood functions using the 'Ψ_{lowest} unbinned' plot (Table 2). Species differed by >11-fold in K_{max}, with no average differences between species from moist and dry habitats, though species differences were significant (considering K_{max} as the mean of K_{leaf} values at Ψ_{leaf} of 0 to -0.5 MPa; ANOVA; $P <0.001$). Species also differed greatly in their vulnerabilities, varying 32-fold in P_{50} and 15-fold in P_{80}, from the most vulnerable species (*H. annuus* and *P. racemosa*) with values less than -1 MPa to the least vulnerable species, *C. diversifolia*, with P_{50} and P_{80} values of -3.54 MPa and -5.25 MPa, respectively (Fig. 2). Species' P_{50} and P_{80} values were strongly correlated (r_p and $r_s=0.88$–0.96, $P <0.01$). Species with greater vulnerability (i.e. with less negative P_{50} and P_{80} values) had steeper vulnerability curve slopes (r_p and $r_s= -0.72$ to -0.83, $P <0.01$; data in Supplementary Table S5 at *JXB* online). On average, species from dry habitats had 2.4- to 2.9-fold more negative P_{50} and P_{80} than species from moist habitats.

Species with lower vulnerability had greater hydraulic safety margins. Thus, safety margins based on P_{50} were negatively correlated with P_{50}, and safety margins based on P_{80} were negatively correlated with both P_{50} and P_{80} (r_p and $r_s= -0.70$ to -0.95; $P <0.05$; data in Supplementary Table S5 at *JXB* online). Safety margins based on P_{50} ranged from -1.9 MPa to 0.17 MPa and were positive for two species (*C. diversifolia* and *H. arbutifolia*); thus, most species lost leaf turgor at lower Ψ_{leaf} than P_{50} as determined using the steady-state method. However, safety margins calculated from P_{80} ranged from -1.7 MPa to 2.7 MPa, and seven species had positive safety margins. Safety margins did not differ between habitat types (*t*-test, $P <0.05$).

Both P_{50} and P_{80} were independent of K_{max} across species ($|r_p|$ and $|r_s|=0.37$–0.62, $P >0.05$).

Recovery of K$_{leaf}$ with leaf rehydration and a new importance for leaf hydraulic vulnerability

Species varied strongly in the ability to recover in K_{leaf} after dehydration below their turgor loss point (such that K_{leaf}

declined by 57–97% depending on species) followed by 1 h rehydration with their petioles under water (Fig. 3). For four species (*C. diversifolia*, *H. annuus*, *L. camara*, and *M. grandiflora*), K_{leaf} increased 2.2- to 2.8-fold (Fig. 3; $P <0.05$); *C. diversifolia* and *M. grandiflora* recovered fully in K_{leaf} to their expected values. Three of these species were moist habitat species (*L. camara*, *H. annuus*, and *M. grandiflora*) and one was a dry habitat species (*C. diversifolia*). The six other species showed no significant recovery. The percentage recovery of K_{leaf} after rehydration did not correlate with K_{max},
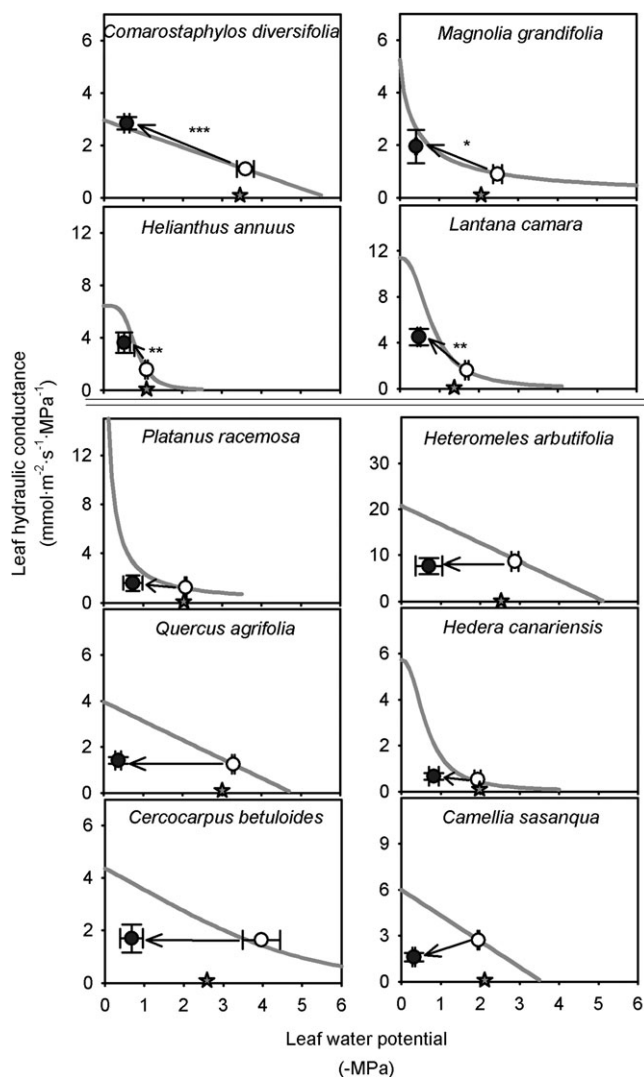
P_{50}, or P_{80} ($P >0.05$; data in Supplementary Table S5 at *JXB* online).

For the six species that did not recover in K_{leaf} with 1 h rehydration, a nearly perfect correlation was found of the ability to maintain K_{leaf} after dehydration and rehydration episodes and low P_{50} and P_{80} (r_s and $r_p= -0.94$ to -0.98; $P <0.005$; Fig. 4). Thus, among the species that did not recover in K_{leaf} with rehydration, a low vulnerability predicted the ability to retain hydraulic capacity despite strong, short-term dynamics in water status.

Testing K_{leaf} recovery during EFM, and its impact on the estimation of hydraulic parameters

No species showed full recovery in K_{leaf} of dehydrated leaves during EFM measurements; for all species there was a persistent impact of dehydration. When the residuals of K_{leaf} against Ψ_{final} were plotted against Ψ_{lowest} (see the Materials and methods), this correlation was significant for seven species ($r_p= -0.49$ to -0.79; $n=25$–74; $P <0.05$; Table 3). For the other three species (*C. sasanqua*, *H. annuus*, and *H. canariensis*) the lack of significant correlation of residuals with Ψ_{lowest} did not imply a complete recovery of K_{leaf} during EFM measurement. In the case of *H. annuus* and *H. canariensis*, the Ψ_{lowest} values were typically the Ψ_{final} values because the leaves dehydrated further during measurement, rather than recovering in Ψ_{leaf}, and, in the case of *C. sasanqua*, because the Ψ_{lowest} correlated with Ψ_{final} ($r_p=0.53$; $P <0.001$) there may not have been sufficient residual variation for a powerful test. There were broadly consistent results in the second analysis of the recovery of K_{leaf} during the EFM measurement (i.e. the calculation of the percentage recovery of K_{leaf} for leaves that rehydrated over the same Ψ_{leaf} interval as the 1 h rehydration experiment). Again there was no evidence for

Fig. 3. Recovery of leaf hydraulic conductance (K_{leaf}) after 1 h rehydration with their petioles under water, for 10 species varying widely in drought tolerance. The grey curves are the best-fit functions of the species' response to dehydration from Fig. 2; open and filled symbols represent the predicted K_{leaf} at the dehydrated leaf water potential, and K_{leaf} after 1h rehydration respectively; stars on the *x*-axis represent the turgor loss point. Species depicted in the upper four panels showed significant recovery in K_{leaf} (*$P=0.04$; **$P=0.001$; ***$P <0.001$); only *C. diversifolia* and *M. grandiflora* showed total recovery. Species depicted in the lower panels showed no significant recovery in K_{leaf}.
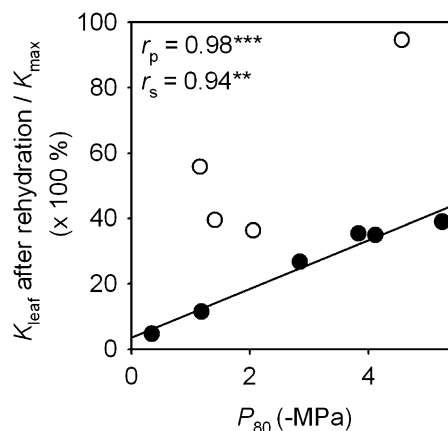
Fig. 4 The ability of hydraulic vulnerability to predict the degree that leaf hydraulic conductance (K_{leaf}) was maintained after strong dehydration and rehydration for 1 h with petiole in water, calculated as K_{leaf} after rehydration divided by maximum K_{leaf} (K_{max}). Filled circles represent species without recovery of K_{leaf} and open circles species that did show recovery of K_{leaf}. The line was fitted only for species without recovery of K_{leaf} (**$P=0.005$; ***$P <0.001$).

Table 3. Results from the tests of the recovery of leaf hydraulic conductance (K_{leaf}) during the evaporative flux method (EFM), and during 1 h rehydration in the dark. In the residual test for recovery during the EFM, significance indicates that K_{leaf} did not fully recover. For the indices of K_{leaf} recovery during the EFM, and during the 1 h rehydration experiments, significance before the comma indicates some degree of significant recovery, and significance after the comma indicates that K_{leaf} did not recover fully (see the Materials and methods).
*P <0.05; **P <0.01; ***P <0.001. NS, non-significant

Species	Residual test for recovery during EFM, R^2 (n)	Index of recovery in K_{leaf} during EFM (% increase)	Index of recovery in K_{leaf} after 1 h rehydration (% increase)
Camellia sasanqua	0.029[NS] (41)	114[NS, **]	58.9[NS, ***]
Cercocarpus betuloides	0.48[***] (70)	119[NS, **]	119[NS, **]
Comarostaphylos diversifolia	0.33[***] (57)	178[**, *]	259[***, NS]
Hedera canariensis	0.036[NS] (41)	159[**, **]	150[NS, ***]
Helianthus annuus	0.017[NS] (36)	124[NS, *]	230[**, *]
Heteromeles arbutifolia	0.62[***] (58)	66.4[NS, *]	79.3[NS, *]
Lantana camara	0.61[***] (25)	161[NS, **]	284[**, **]
Magnolia grandiflora	0.24[*] (74)	158[**, ***]	218[*, NS]
Platanus racemosa	0.35[***] (38)	104[NS, *]	130[NS, *]
Quercus agrifolia	0.38[***] (46)	72.2[NS, **]	113[NS, ***]

total recovery of K_{leaf}. There was a significant partial recovery of K_{leaf} in 3/10 species (P <0.007; Table 3), with K_{leaf} increasing by 158–178%. Across species, the recovery of K_{leaf} during the EFM was positively correlated with that observed after 1 h rehydration (r_p and r_s=0.83–0.84; P <0.05). The percentage recovery of K_{leaf} during the EFM was 13% lower on average than that after 1 h rehydration, consistent with the leaf rehydrating for a shorter period of time, under sub-atmospheric pressure (paired *t*-test; P=0.04).

Given that three species indicated partial K_{leaf} recovery during EFM measurement, an analysis was made of its potential influence on derived vulnerability parameters (see the Materials and methods). Re-calculating these species' K_{max}, P_{50}, and P_{80} values while considering the partial K_{leaf} recovery produced values that were correlated with those determined using both the 'Ψ_{lowest} unbinned' and 'Ψ_{lowest} binned' plots (r_s and r_p=0.57–0.99; P <0.001–0.09), indicating that species comparisons using those vulnerability plots are robust even despite partial K_{leaf} recovery. However, the re-calculated parameters accounting for partial recovery did not correlate with those determined using the 'Ψ_{final}' plot (r_s and r_p=0.08–0.30; P=0.16–0.83).

Discussion

The new steady-state EFM developed for determining the hydraulic vulnerability of leaves acclimated to high irradiance allowed an independent confirmation and extension of key relationships first shown using rehydration methods. Additionally, refined statistical methods for analysing vulnerability data allowed fitting of the appropriate function for each species and considering the effect of recovery during the measurement. These approaches showed novel variation among species in leaf vulnerability, and relationships with species' habitat. Further, rehydration experiments quantifying the rapid recovery of K_{leaf} after dehydration indicated novel species variation, and a new role for leaf vulnerability in

determining function after episodes of dehydration and rehydration. This work provided new insights into the vulnerability response, and will additionally enable higher resolution in future work investigating the underlying mechanisms for leaf hydraulic vulnerability.

Species' differences in K_leaf decline and potential mechanisms

Species differed strikingly in their vulnerability parameters P_{50} and P_{80}, and in the shape of their vulnerability curves. Notably, because species varied strongly in initial K_{leaf} values (K_{max}) and in the steepness of their decline in K_{leaf}, P_{80} was useful to allow comparison of species' vulnerabilities at a similar stage of their trajectory, namely after the steepest decline phase (Fig. 2), whereas P_{50} values often occurred in the middle of the steepest decline, which for some species occurred at very high Ψ_{leaf}. For such species the P_{50} may not be an effective index of drought resistance. Further, it is noted that several species (e.g. *P. racemosa*) had very high K_{max}, with substantial K_{leaf} decline before Ψ_{leaf} reached –0.5 MPa. Though part of the true range of leaf hydraulic behaviour in such species, such very high K_{leaf} values are outside of the range found in nature, as they would not occur for leaves transpiring *in vivo*, in which the soil and plant hydraulic resistance would cause a further Ψ_{leaf} drop not experienced by leaves in the EFM. Species with such steep, non-linear decline were typical of moist habitat species, whereas species with shallow, linear declines were associated with dry habitats.

The K_{leaf} decline during dehydration arises due to loss of hydraulic conductance in the petiole and/or vein xylem, and/or the extra-xylem pathways (Table 1). The importance of (i) cavitation due to air seeding in major veins leading to subsequent embolism was supported by studies showing ultra-acoustic emissions that may reflect cavitation events (Kikuta *et al.*, 1997; Salleo *et al.*, 2000; Johnson *et al.*, 2009a), as well as dye and cryo-scanning electron

microscope studies showing embolism in vein xylem (Salleo *et al.*, 2001; Nardini *et al.*, 2003, 2008; Johnson *et al.*, 2009*a*), measurement of relatively low air seeding pressures in the leaf petiole and midrib (Choat *et al.*, 2005), and a correlation across species of hydraulic vulnerability with low major vein length per leaf area, as such leaves have less xylem redundancy to protect from the impact of embolism (Scoffoni *et al.*, 2011). Another mechanism may be (ii) the collapse of xylem conduits in the leaf veins; indeed xylem cell collapse has been found for tracheids in the vein of pine needles and in the transfusion tissue of a tropical conifer, at Ψ_{leaf} values as high as –1.5 MPa, in advance of cavitation (Cochard *et al.*, 2004; Brodribb and Holbrook, 2005). Indeed, xylem cell collapse has been hypothesized to occur in the minor vein xylem in angiosperms too, but has not yet been visualized directly (Blackman *et al.*, 2010). Additionally, K_{leaf} decline might relate to (iii) the loss of turgor in living cells in the extra-xylem flow pathways (Brodribb and Holbrook, 2006), in particular the cells of the bundle sheath, mesophyll, and epidermis, which may shrink with walls retracting, and/or may undergo plasmolysis. Tissues with low solute potential, such as bundle sheath, might lose turgor in advance of the mesophyll (Giles *et al.*, 1974; Palta and Leestadelmann, 1983; Nonami and Schulze, 1989; Canny and Huang, 2006). Such changes in cell volume and turgor may alter the flow pathways, and additionally reduce membrane permeability, for example via deactivation of aquaporins (Kim and Steudle, 2007). A final mechanism for the K_{leaf} decline especially in well-hydrated leaves is (iv) the evaporation of liquid water in the cells walls during transpiration, leaving walls moist but with empty pores and thus lower permeability (Kim and Steudle, 2007; Lee *et al.*, 2009; Voicu *et al.*, 2009).

The shapes of functions fitted to K_{leaf} data from the present study using maximum likelihood provide several key insights and hypotheses for the action of these mechanisms and point to a diversity in specific impacts across species. Given that embolism or collapse of vein xylem conduits is a principal driver of the K_{leaf} decline, the linear decline observed for four species implies that air seeding or collapse begins at high Ψ_{leaf} for these species (see references in Table 1). The linear decline also implies that conduits of different sizes tend to have approximately equal distributions of air seeding pressures and tendencies to collapse, and/or that a high major vein density provides redundancy that protects the leaf from a disproportionate effect of cavitation of the major vein xylem. A linear decline of K_{leaf} would also be consistent with a direct role for loss in mesophyll, epidermis, or bundle sheath cell volume or turgor, or the number of water pathways through cell walls declining approximately linearly with Ψ_{leaf} above the turgor loss point (Table 1). The logistic decline observed in five species and sigmoidal decline in *C. betuloides* indicate a qualitative difference. Given that xylem cavitation and/or collapse play a principal role, for these species the steep decline at high Ψ_{leaf} that slows with ongoing dehydration is consistent with an unequal distribution of air seeding pressures, for example the larger vessels that confer the

bulk of vein xylem conductivity cavitating and/or collapsing first, and smaller vessels having lower air seeding pressures or wall strength and losing function at lower Ψ_{leaf} (Table 1). A disproportionate decline at high Ψ_{leaf} could also relate to species having low major vein densities; and thus, embolism occurring early in these veins, would result in substantial declines in K_{leaf} (Table 1). If losses in cell permeability are important, the disproportionate decline at high Ψ_{leaf} could relate to a strong sensitivity of K_{leaf} to losses in volume in particular cells, with low solute potential, for example bundle sheath cells, that may shrink at high Ψ_{leaf} and/or undergo aquaporin deactivation (Table 1). If losses of cell wall pathways contribute to the loss of K_{leaf}, a disproportionate decline at high Ψ_{leaf} would be consistent with the cell walls behaving as observed for other porous media that show non-linear declines in conductivity with declining water potential, for example soil (Laio *et al.*, 2001). The species variation in vulnerability curves points to the critical importance of research to disentangle the specific mechanisms of K_{leaf} decline for given species. Notably, previous work has shown species variation in partitioning of hydraulic resistance between petiole and lamina, and among vein orders, and between the vein xylem and extra-xylem pathways (Trifilo *et al.*, 2003*b*; Sack *et al.*, 2004, 2005). These species differences would also result in variation in the important mechanisms underlying sensitivity to hydraulic decline because K_{leaf} would be most sensitive to declines in conductance in the component that accounted for the greatest part of the leaf resistance (Scoffoni *et al.*, 2011).

In this study the focus was on on the response of K_{leaf} to dehydration under high irradiance. It is noted that many species show an increase of K_{leaf} under high irradiance, and this response may interact with the response to dehydration (Kim and Steudle, 2007; Lee *et al.*, 2009; Voicu *et al.*, 2009). The decline in conductance under low irradiance occurs in the extra-xylem tissues (Nardini *et al.*, 2005); thus, under low irradiance, the extra-xylem tissues would account for a greater proportion of leaf resistance, and cavitation or collapse of vein xylem would have a lesser impact on K_{leaf}, and any reduction in the permeability of extra-xylem tissues due to dehydration would have a stronger impact (Nardini *et al.*, 2005; Scoffoni *et al.*, 2008; Voicu *et al.*, 2008). The interaction of the light and dehydration responses of K_{leaf} is an important area for future investigation.

Quantifying the vulnerability of K$_{leaf}$: importance and limitations of the steady-state method

Since it is not yet possible to determine K_{leaf} directly across a full range of Ψ_{leaf} *in vivo*, hydraulic methods have been applied to excised leaves. The EFM is the latest of several approaches to measuring K_{leaf} vulnerability on excised leaves. These methods have advantages over indirect methods, such as the audio method, which registers amplified ultrasonic acoustic emissions (UAEs) within drying plant tissue, hypothesized to arise from cavitation (Milburn and Johnson, 1966; Tyree and Dixon, 1983, 1986; Kikuta *et al.*, 1997; Johnson *et al.*, 2009*a*), or visual

methods using dye or cryo-scanning electron microscopy that directly demonstrate embolism in dehydrated leaves (Salleo *et al.*, 2000, 2001), and collapse of conduits in dehydrated conifer leaves (Cochard *et al.*, 2004; Brodribb and Holbrook, 2005), because these methods do not provide information of possible extra-xylem decline, or directly measure hydraulic vulnerability. Hydraulic methods applied to excised leaves include, in addition to the EFM, the high pressure flowmeter (Nardini *et al.*, 2001), the vacuum pump method (Lo Gullo *et al.*, 2003), and the RKM, most frequently used for determining leaf hydraulic vulnerability, which estimates K_{leaf} from the uptake of water during rehydration by analogy to the charging of a capacitor in series with a resistor (Brodribb and Holbrook, 2003*a*, 2004*a*, *b*, 2006; Woodruff *et al.*, 2007, 2008; Hao *et al.*, 2008; Blackman *et al.*, 2009; Brodribb and Cochard, 2009; Johnson *et al.*, 2009*a*, *b*; Saha *et al.*, 2009; Blackman and Brodribb, 2011). As described in the Introduction, these methods all have merits and disadvantages. The steady-state EFM is independent of the RKM, and here it confirmed and extended key findings.

Several limitations of the EFM applied to excised leaves apply equally to the other methods for leaf vulnerability. These methods cannot assess the decline of K_{leaf} and Ψ_{leaf} that occurs *in vivo*, when xylem water is under tension, and leaf cells are equilibrated at very low water potentials; the xylem cells may be collapsed, leaf cells shrunken, and aquaporins inactivated (Cochard *et al.*, 2002, 2004; Brodribb and Holbrook, 2005, 2006; Canny and Huang, 2006). Excising the leaf under water relieves the tension, and some of these effects might be reversed rapidly. Discovery of such effects would require new *in vivo* methods for measuring K_{leaf} decline. In the meantime, vulnerability measured on excised leaves must be considered as conservative, because these methods measure only the K_{leaf} decline that is not instantly recoverable, for example embolism in veins, which may require many minutes to hours of low tension and active processes to recover (Tyree and Zimmermann, 2002; Bucci *et al.*, 2003; Trifilo *et al.*, 2003*a*), and persistent effects on living tissues. Further, all the methods may be affected by recovery of K_{leaf} with rehydration during the measurement itself, but the analysis in this study showed that comparative estimates of hydraulic vulnerability remained robust despite such recovery.

Linkage of vulnerability with drought sensitivity

Species of dry habitats had lower vulnerability (i.e. lower P_{50} and P_{80}) than species of moist habitat. This finding was consistent with that of a study of Australian species using the RKM (Blackman *et al.*, 2010), here extended with the steady-state method to a set of species very diverse in drought tolerance. This study also confirmed no trade-off across species between K_{max} and hydraulic vulnerability, as previously reported using RKM (Blackman *et al.*, 2010) and in a meta-analysis combining data collected with different methods (Sack and Holbrook, 2006), a relationship frequently found for stems (Tyree and Zimmermann, 2002;

Maherali *et al.*, 2004; Meinzer *et al.*, 2010). Notably, species from dry and moist habitats did not differ on average in their K_{max}. This finding is consistent with multiple types of adaptation to drought. Some drought-tolerant species use water sparingly via low maximum rates of gas exchange, consistent with low K_{max}, while others conduct rapid gas exchange when water is available, consistent with high K_{max}, and then 'gear-down' during shortage, (Maximov, 1931; Grubb, 1998), as illustrated by species such as *H. arbutifolia* (maximum photosynthetic rate of 14 μmol CO_2 m^{-2} s^{-1}; Valladares and Pearcy, 1997).

It was also found that across species P_{50} and P_{80} were strongly correlated with the bulk leaf turgor loss point (π_{TLP}) and osmotic potential (Scoffoni *et al.*, 2011; Fig. 5). This finding confirmed and extended the correlation previously reported between P_{50} and π_{TLP} for 19 species using the RKM (Blackman *et al.*, 2010). A low π_{TLP} might confer resistance to K_{leaf} decline directly, if it allows cells to preserve their structural integrity at lower bulk Ψ_{leaf} (Blackman *et al.*, 2010). Previous work has demonstrated the heterogeneity of solute potential and across lamina locations and tissues (Slavik, 1959; Nonami and Schulze, 1989; Koroleva *et al.*, 1997, 2002), and the correlation with vulnerability might be even stronger with the turgor loss point of individual tissues important in the water flow pathways, for example the bundle sheath, rather than for the bulk leaf.
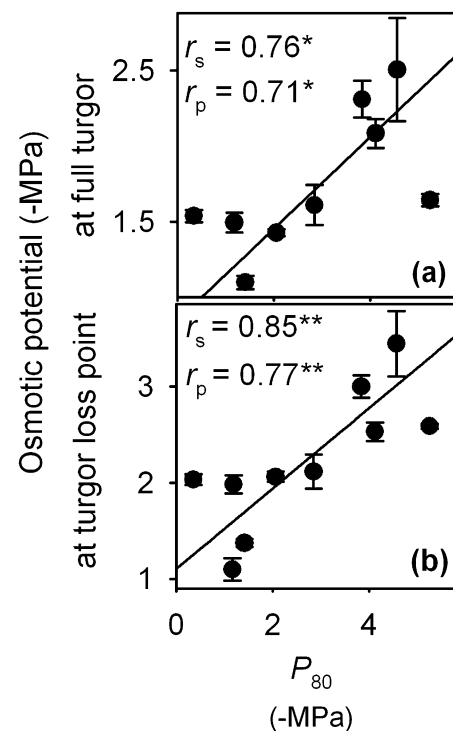

Fig. 5. Correlation of the leaf water potential at 80% loss of leaf hydraulic conductance (P_{80}) with osmotic potentials (a) at full turgor (π_o) and (b) at turgor loss point (π_{TLP}), for 10 species of a wide range of drought tolerance. Fitted standard major axes: (a) $\pi_o = 0.30 \times P_{80} + 0.85$; (b) $\pi_{TLP} = 0.42 \times P_{80} + 1.1$. Data for π_o and π_{TLP} are from Scoffoni *et al.* (2011).

One consequence of the correlation of vulnerability and π_{TLP} is a mechanism for inducing protective stomatal closure in drought-sensitive species (Brodribb and Cochard, 2009; Hao *et al.*, 2010). The narrow safety margins found in this study were consistent with past studies showing angiosperms often operating at close to cavitation thresholds (Lo Gullo *et al.*, 2003; Brodribb and Holbrook, 2004a, b) in contrast to conifers and ferns which can have wide safety margins (Brodribb and Holbrook, 2004b). Declines in K_{leaf} accelerate further declines in Ψ_{leaf} at a given transpiration rate, and guard cells lose turgor against the background of epidermal cell pressure (Franks and Farquhar, 1999; Damour *et al.*, 2010). After that point, cuticular water loss would lead to slower declines of Ψ_{leaf} and of K_{leaf} (Pasquet-Kok *et al.*, 2010). In contrast, in species with low hydraulic vulnerability, the maintenance of K_{leaf} would allow stomata to remain open without desiccating the mesophyll during diurnal water stress or soil drought (Brodribb and Holbrook, 2003a). This contribution of K_{leaf} sensitivity to stomatal control is important in whole-plant drought tolerance (Brodribb and Cochard, 2009; Blackman *et al.*, 2010).

Species differences in K_{leaf} recovery and a new importance of resistance to K_{leaf} decline

A strong, novel variation across species was found in the ability of dehydrated leaves to recover rapidly in K_{leaf} with 1 h of rehydration. Six species showed no recovery and four increased in K_{leaf} by 2.5- to 2.8-fold. This study thus partially confirmed one previous report of a complete recovery for sunflower (Trifilo *et al.*, 2003a). Typically K_{leaf} did not fully recover after 1 h rehydration, indicating a partial irreversibility consistent with embolisms that require refilling, or losses of cell permeability that might require energy transduction for recovery (Bucci *et al.*, 2003).

The present data on vulnerability and recovery highlighted a new importance for leaf hydraulics in determining performance with changing plant water status. A recent meta-analysis of data for 31 species found that at minimum daily Ψ_{leaf}, species varied greatly in their K_{leaf} decline, with roughly half the species being below P_{50} (Johnson *et al.*, 2009b). Our study showed that among species that did not recover rapidly in K_{leaf} with rehydration, a low hydraulic vulnerability conferred the ability to maintain K_{leaf} at a high value through both dehydration and rehydration. Species resistant to hydraulic decline could thus maintain K_{leaf} at high levels despite transient but severe dynamics in Ψ_{leaf}, and gain a benefit in maintaining performance during diurnal water stress or soil drought. These findings are consistent with the correlation of low leaf hydraulic vulnerability and the ability of severely droughted plants to recover in transpiration after rewatering (Blackman *et al.*, 2009; Brodribb and Cochard, 2009). Tests are needed of the degree that rapid leaf hydraulic recovery, as shown in this study, contributes to whole-plant hydraulic recovery and tolerance of dynamic water regimes.

Supplementary data

Supplementary data are available at *JXB* online.

Table S1. A summary of previous studies of leaf hydraulic vulnerability on whole leaves, indicating the various methods used, the different functions fitted to the data, and whether the data were binned or not before line fitting.

Table S2. Minimum and maximum transpirational flow rates (E) for each species measured with the evaporative flux method and corresponding estimated stomatal conductances (g), and cuticular conductances for these species.

Table S3. Parameters for the decline of leaf hydraulic conductance (K_{leaf}) with declining leaf water potential for 10 species, fitted with four different functions, R^2 for observed values plotted against predicted values from the fitted function, and values for the Akaike Information Criterion (AIC). For each function, three plots were tested for K_{leaf} against leaf water potential: (1) 'Ψ_{lowest} unbinned'; (2) 'Ψ_{lowest} binned'; (3) and 'Ψ_{final}' (see the Materials and methods for additional information).

Table S4. Parameters of leaf hydraulic vulnerability curves (K_{max}, P_{50}, and P_{80}) determined by fitting four functions to the data for each species (linear, sigmoidal, logistic, and exponential) and using three kinds of plots 'Ψ_{owest} unbinned', 'Ψ_{lowest} binned', and' Ψ_{final}').

Table S5. Species means ±SEs for leaf hydraulic vulnerability parameters and pressure–volume parameters for 10 species ranging widely in drought tolerance.

Acknowledgements

References

Blackman CJ, Brodribb TJ. 2011. Two measures of leaf capacitance: insights into the water transport pathway and hydraulic conductance in leaves. *Functional Plant Biology* **38,** 118–126.

Blackman CJ, Brodribb TJ, Jordan GJ. 2009. Leaf hydraulics and drought stress: response, recovery and survivorship in four woody temperate plant species. *Plant, Cell and Environment* **32,** 1584–1595.

Blackman CJ, Brodribb TJ, Jordan GJ. 2010. Leaf hydraulic vulnerability is related to conduit dimensions and drought resistance across a diverse range of woody angiosperms. *New Phytologist* **188,** 1113–1123.

Boyer JS. 1967. Leaf water potentials measured with a pressure chamber. *Plant Physiology* **42,** 133–137.

Brodribb TJ, Blackman CJ, **Prometheus Wiki contributors**. PROTOCOL: non-steady state rehydration to determine leaf hydraulic conductance, vulnerability and capacitance. *PrometheusWiki.* Retrieved 02June2011, from

http://www.publish.csiro.au/prometheuswiki/tiki-pagehistory.php?page=PROTOCOL Non-steady state rehydration to determine leaf hydraulic conductance, vulnerability and capacitance&preview=.

Brodribb TJ, Cochard H. 2009. Hydraulic failure defines the recovery and point of death in water-stressed conifers. *Plant Physiology* **149,** 575–584.

Brodribb TJ, Feild TS, Sack L. 2010. Viewing leaf structure and evolution from a hydraulic perspective. *Functional Plant Biology* **37,** 488–498.

Brodribb TJ, Holbrook NM. 2003a. Stomatal closure during leaf dehydration, correlation with other leaf physiological traits. *Plant Physiology* **132,** 2166–2173.

Brodribb TJ, Holbrook NM. 2003b. Changes in leaf hydraulic conductance during leaf shedding in seasonally dry tropical forest. *New Phytologist* **158,** 295–303.

Brodribb TJ, Holbrook NM. 2004a. Diurnal depression of leaf hydraulic conductance in a tropical tree species. *Plant, Cell and Environment* **27,** 820–827.

Brodribb TJ, Holbrook NM. 2004b. Stomatal protection against hydraulic failure: a comparison of coexisting ferns and angiosperms. *New Phytologist* **162,** 663–670.

Brodribb TJ, Holbrook NM. 2005. Water stress deforms tracheids peripheral to the leaf vein of a tropical conifer. *Plant Physiology* **137,** 1139–1146.

Brodribb TJ, Holbrook NM. 2006. Declining hydraulic efficiency as transpiring leaves desiccate: two types of response. *Plant, Cell and Environment* **29,** 2205–2215.

Brodribb TJ, Holbrook NM. 2007. Forced depression of leaf hydraulic conductance in situ: effects on the leaf gas exchange of forest trees. *Functional Ecology* **21,** 705–712.

Bucci SJ, Scholz FG, Goldstein G, Meinzer FC, Sternberg LDL. 2003. Dynamic changes in hydraulic conductivity in petioles of two savanna tree species: factors and mechanisms contributing to the refilling of embolized vessels. *Plant, Cell and Environment* **26,** 1633–1645.

Buck AL. 1981. New equations for computing vapor-pressure and enhancement factor. *Journal of Applied Meteorology* **20,** 1527–1532.

Burnham KP, Anderson DR. 2002. *Model selection and multimodel inference*, 2nd edn. New York: Springer.

Burnham KP, Anderson DR. 2004. Multimodel inference—understanding AIC and BIC in model selection. *Sociological Methods and Research* **33,** 261–304.

Canny MJ, Huang CX. 2006. Leaf water content and palisade cell size. *New Phytologist* **170,** 75–85.

Chen JW, Zhang Q, Li XS, Cao KF. 2009. Independence of stem and leaf hydraulic traits in six Euphorbiaceae tree species with contrasting leaf phenology. *Planta* **230,** 459–468.

Choat B, Lahr EC, Melcher P, Zwieniecki MA, Holbrook NM. 2005. The spatial pattern of air seeding thresholds in mature sugar maple trees. *Plant, Cell and Environment* **28,** 1082–1089.

Cochard H, Coll L, Le Roux X, Ameglio T. 2002. Unraveling the effects of plant hydraulics on stomatal closure during water stress in walnut. *Plant Physiology* **128,** 282–290.

Cochard H, Froux F, Mayr FFS, Coutand C. 2004. Xylem wall collapse in water-stressed pine needles. *Plant Physiology* **134,** 401–408.

Cochard H, Venisse JS, Barigah TS, Brunel N, Herbette S, Guilliot A, Tyree MT, Sakr S. 2007. Putative role of aquaporins in variable hydraulic conductance of leaves in response to light. *Plant Physiology* **143,** 122–133.

Cowan IR. 1972. Electrical analog of evaporation from, and flow of water in plants. *Planta* **106,** 221–226.

Croat TB. 1978. *Flora of Barro Colorado Island*. California: Stanford University Press.

Damour G, Simonneau T, Cochard H, Urban L. 2010. An overview of models of stomatal conductance at the leaf level. *Plant, Cell and Environment* **33,** 1419–1438.

Domec JC, Lachenbruch B, Meinzer FC. 2006. Bordered pit structure and function determine spatial patterns of air-seeding thresholds in xylem of Douglas-fir (*Pseudotsuga menziesii*; Pinaceae) trees. *American Journal of Botany* **93,** 1588–1600.

eFloras. 2008. Flora of North America. *Missouri Botanical Garden & Harvard University Herbaria* Vol. 2010. St. Louis, MO and Cambridge, MA http://www.efloras.org/.

Franks PJ, Farquhar GD. 1999. A relationship between humidity response, growth form and photosynthetic operating point in C-3 plants. *Plant, Cell and Environment* **22,** 1337–1349.

Giles KL, Beardsel MF, Cohen D. 1974. Cellular and ultrastructural changes in mesophyll and bundle sheath-cells of maize in response to water stress. *Plant Physiology* **54,** 208–212.

Grubb PJ. 1998. A reassessment of the strategies of plants which cope with shortages of resources. *Perspectives in Plant Ecology Evolution and Systematics* **1,** 3–31.

Hao GY, Hoffmann WA, Scholz FG, Bucci SJ, Meinzer FC, Franco AC, Cao KF, Goldstein G. 2008. Stem and leaf hydraulics of congeneric tree species from adjacent tropical savanna and forest ecosystems. *Oecologia* **155,** 405–415.

Hao GY, Sack L, Wang AY, Cao KF, Goldstein G. 2010. Differentiation of leaf water flux and drought tolerance traits in hemiepiphytic and non-hemiepiphytic *Ficus* tree species. *Functional Ecology* **24,** 731–740.

Iovi K, Kolovou C, Kyparissis A. 2009. An ecophysiological approach of hydraulic performance for nine Mediterranean species. *Tree Physiology* **29,** 889–900.

Johansson I, Karlsson M, Shukla VK, Chrispeels MJ, Larsson C, Kjellbom P. 1998. Water transport activity of the plasma membrane aquaporin PM28A is regulated by phosphorylation. *The Plant Cell* **10,** 451–459.

Johnson DM, Meinzer FC, Woodruff DR, McCulloh KA. 2009a. Leaf xylem embolism, detected acoustically and by cryo-SEM, corresponds to decreases in leaf hydraulic conductance in four evergreen species. *Plant, Cell and Environment* **32,** 828–836.

Johnson DM, Woodruff DR, McCulloh KA, Meinzer FC. 2009b. Leaf hydraulic conductance, measured in situ, declines and recovers daily: leaf hydraulics, water potential and stomatal conductance in four temperate and three tropical tree species. *Tree Physiology* **29,** 879–887.

Kikuta SB, LoGullo MA, Nardini A, Richter H, Salleo S. 1997. Ultrasound acoustic emissions from dehydrating leaves of deciduous and evergreen trees. *Plant, Cell and Environment* **20,** 1381–1390.

Kim YX, Steudle E. 2007. Light and turgor affect the water permeability (aquaporins) of parenchyma cells in the midrib of leaves of Zea mays. *Journal of Experimental Botany* **58,** 4119–4129.

Kitamura S, Murata G. 1979. *Colored illustrations of woody plants of Japan* Revised editions, Vol. II. Osaka: Hoikusha, 158–159.

Koroleva OA, Farrar JF, Tomos AD, Pollock CJ. 1997. Patterns of solute in individual mesophyll, bundle sheath and epidermal cells of barley leaves induced to accumulate carbohydrate. *New Phytologist* **136,** 97–104.

Koroleva OA, Tomos AD, Farrar J, Pollock CJ. 2002. Changes in osmotic and turgor pressure in response to sugar accumulation in barley source leaves. *Planta* **215,** 210–219.

Kubiske ME, Abrams MD. 1990. Pressure–volume relationships in non-rehydrated tissue at various water deficits. *Plant, Cell and Environment* **13,** 995–1000.

Laio F, Porporato A, Ridolfi L, Rodriguez-Iturbe I. 2001. Plants in water-controlled ecosystems: active role in hydrologic processes and response to water stress—II. Probabilistic soil moisture dynamics. *Advances in Water Resources* **24,** 707–723.

Lee SH, Chung GC, Zwiazek JJ. 2009. Effects of irradiance on cell water relations in leaf bundle sheath cells of wild-type and transgenic tobacco (*Nicotiana tabacum*) plants overexpressing aquaporins. *Plant Science* **176,** 248–255.

Lo Gullo MA, Nardini A, Trifilo P, Salleo S. 2003. Changes in leaf hydraulics and stomatal conductance following drought stress and irrigation in *Ceratonia siliqua* (Carob tree). *Physiologia Plantarum* **117,** 186–194.

Maherali H, Pockman WT, Jackson RB. 2004. Adaptive variation in the vulnerability of woody plants to xylem cavitation. *Ecology* **85,** 2184–2199.

Maximov NA. 1931. The physiological significance of the xeromorphic structure of plants. *Journal of Ecology* **19,** 273–282.

Meinzer FC, McCulloh KA, Lachenbruch B, Woodruff DR, Johnson DM. 2010. The blind men and the elephant: the impact of context and scale in evaluating conflicts between plant hydraulic safety and efficiency. *Oecologia* **164,** 287–296.

Milburn JA, Johnson RPC. 1966. Conductance of sap. 2. Detection of vibrations produced by sap cavitation in *Ricinus xylem*. *Planta* **69,** 43–52.

Miyazawa S, Yoshimura S, Shinzaki Y, Maeshima M, Miyake C. 2008. Deactivation of aquaporins decreases internal conductance to CO_2 diffusion in tobacco leaves grown under long-term drought. *Functional Plant Biology* **35,** 553–564.

Nardini A, Ramani M, Gortan E, Salleo S. 2008. Vein recovery from embolism occurs under negative pressure in leaves of sunflower (*Helianthus annuus*). *Physiologia Plantarum* **133,** 755–764.

Nardini A, Salleo S, Andri S. 2005. Circadian regulation of leaf hydraulic conductance in sunflower (*Helianthus annuus* L. cv Margot). *Plant, Cell and Environment* **28,** 750–759.

Nardini A, Salleo S, Raimondo F. 2003. Changes in leaf hydraulic conductance correlate with leaf vein embolism in *Cercis siliquastrum* L. *Trees-Structure and Function* **17,** 529–534.

Nardini A, Tyree MT, Salleo S. 2001. Xylem cavitation in the leaf of *Prunus laurocerasus* and its impact on leaf hydraulics. *Plant Physiology* **125,** 1700–1709.

Neufeld HS, Grantz DA, Meinzer FC, Goldstein G, Crisosto GM, Crisosto C. 1992. Genotypic variability in vulnerability of leaf xylem to cavitation in water-stressed and well-irrigated sugarcane. *Plant Physiology* **100,** 1020–1028.

Nonami H, Schulze ED. 1989. Cell water potential, osmotic potential, and turgor in the epidermis and mesophyll of transpiring leaves. Combined measurements with the cell pressure probe and nanoliter osmometer. *Planta* **177,** 35–46.

North GB, Nobel PS. 2000. Heterogeneity in water availability alters cellular development and hydraulic conductivity along roots of a desert succulent. *Annals of Botany* **85,** 247–255.

Palta JP, Leestadelmann OY. 1983. Vacuolated plant-cells as ideal osmometer—reversibility and limits of plasmolysis, and estimation of protoplasm volume in control and water-stress tolerant cells. *Plant, Cell and Environment* **6,** 601–610.

Pammenter NW, Vander Willigen C. 1998. A mathematical and statistical analysis of the curves illustrating vulnerability of xylem to cavitation. *Tree Physiology* **18,** 589–593.

Pasquet-Kok J, Creese C, Sack L. 2010. Turning over a new 'leaf': multiple functional significances of leaves versus phyllodes in Hawaiian *Acacia koa*. *Plant, Cell and Environment* **33,** 2084–2100.

Pieruschka R, Huber G, Berry JA. 2010. Control of transpiration by radiation. *Proceedings of the National Academy of Sciences, USA* **107,** 13372–13377.

Sack L, Cowan PD, Jaikumar N, Holbrook NM. 2003. The 'hydrology' of leaves: co-ordination of structure and function in temperate woody species. *Plant, Cell and Environment* **26,** 1343–1356.

Sack L, Holbrook NM. 2006. Leaf hydraulics. *Annual Review of Plant Biology* **57,** 361–381.

Sack L, Melcher PJ, Liu WH, Middleton E, Pardee T. 2006. How strong is intracanopy leaf plasticity in temperate deciduous trees? *American Journal of Botany* **93,** 829–839.

Sack L, Melcher PJ, Zwieniecki MA, Holbrook NM. 2002. The hydraulic conductance of the angiosperm leaf lamina: a comparison of three measurement methods. *Journal of Experimental Botany* **53,** 2177–2184.

Sack L, Streeter CM, Holbrook NM. 2004. Hydraulic analysis of water flow through leaves of sugar maple and red oak. *Plant Physiology* **134,** 1824–1833.

Sack L, Tyree MT. 2005. Leaf hydraulics and its implications in plant structure and function. In: Holbrook NM, Zweiniecki MA, eds. *Vascular transport in plants*. Oxford: Elsevier/Academic Press, 93–114.

Sack L, Tyree MT, Holbrook NM. 2005. Leaf hydraulic architecture correlates with regeneration irradiance in tropical rainforest trees. *New Phytologist* **167,** 403–413.

Saha S, Holbrook NM, Montti L, Goldstein G, Cardinot GK. 2009. Water relations of *Chusquea ramosissima* and *Merostachys claussenii* in Iguazu National Park, Argentina. *Plant Physiology* **149,** 1992–1999.

Salleo S, Lo Gullo MA, Raimondo F, Nardini A. 2001. Vulnerability to cavitation of leaf minor veins: any impact on leaf gas exchange? *Plant, Cell and Environment* **24,** 851–859.

Salleo S, Nardini A, Pitt F, Lo Gullo MA. 2000. Xylem cavitation and hydraulic control of stomatal conductance in laurel (*Laurus nobilis* L.). *Plant, Cell and Environment* **23,** 71–79.

Scoffoni C, Pou A, Aasamaa K, Sack L. 2008. The rapid light response of leaf hydraulic conductance: new evidence from two experimental methods. *Plant, Cell and Environment* **31,** 1803–1812.

Scoffoni C, Rawls M, McKown A, Cochard H, Sack L. 2011. Decline of leaf hydraulic conductance with dehydration: relationship to leaf size and venation architecture. *Plant Physiology* **156,** 832–843.

Sellin A, Kupper P. 2007. Temperature, light and leaf hydraulic conductance of little-leaf linden (*Tilia cordata*) in a mixed forest canopy. *Tree Physiology* **27,** 679–688.

Sellin A, Ounapuu E, Kupper P. 2008. Effects of light intensity and duration on leaf hydraulic conductance and distribution of resistance in shoots of silver birch (*Betula pendula*). *Physiologia Plantarum* **134,** 412–420.

Slavik B. 1959. Gradients of osmotic pressure of cell sap in the area of one leaf blade. *Biologia Plantarum* **1,** 39–47.

Sokal RR, Rohlf FJ. 1995. *Biometry: the principles and practice of statistics in biological research*, 3rd edn. New York: W.H. Freeman and Company.

Trifilo P, Gasco A, Raimondo F, Nardini A, Salleo S. 2003*a*. Kinetics of recovery of leaf hydraulic conductance and vein functionality from cavitation-induced embolism in sunflower. *Journal of Experimental Botany* **54,** 2323–2330.

Trifilo P, Nardini A. 2003*b*. Lo Gullo MA, Salleo S. Vein cavitation and stomatal behaviour of sunflower (*Helianthus annuus*) leaves under water limitation. *Physiologia Plantarum* **119,** 409–417.

Tyree MT, Dixon MA. 1983. Cavitation events in *Thuja occidentalis* L. Ultrasonic acoustic emissions from the sapwood can be measured. *Plant Physiology* **72,** 1094–1099.

Tyree MT, Dixon MA. 1986. Water-stress induced cavitation and embolism in some woody plants. *Physiologia Plantarum* **66,** 397–405.

Tyree MT, Nardini A, Salleo S, Sack L, El Omari B. 2005. The dependence of leaf hydraulic conductance on irradiance during HPFM measurements: any role for stomatal response? *Journal of Experimental Botany* **56,** 737–744.

Tyree MT, Zimmermann MH. 2002. *Xylem structure and the ascent of sap*. Berlin: Springer.

Valladares F, Pearcy RW. 1997. Interactions between water stress, sun-shade acclimation, heat tolerance and photoinhibition in the sclerophyll *Heteromeles arbutifolia*. *Plant, Cell and Environment* **20,** 25–36.

Voicu MC, Cooke JEK, Zwiazek JJ. 2009. Aquaporin gene expression and apoplastic water flow in bur oak (*Quercus macrocarpa*) leaves in relation to the light response of leaf hydraulic conductance. *Journal of Experimental Botany* **60,** 4063–4075.

Voicu MC, Zwiazek JJ, Tyree MT. 2008. Light response of hydraulic conductance in bur oak (*Quercus macrocarpa*) leaves. *Tree Physiology* **28,** 1007–1015.

Warton DI, Wright IJ, Falster DS, Westoby M. 2006. Bivariate line-fitting methods for allometry. *Biological Reviews* **81,** 259–291.

Weast RC, ed. 1974. *Handbook of chemistry and physics*, 54th edn. Cleveland, OH: CRC Press.

Woodruff DR, McCulloh KA, Warren JM, Meinzer FC, Lachenbruch B. 2007. Impacts of tree height on leaf hydraulic architecture and stomatal control in Douglas-fir. *Plant, Cell and Environment* **30,** 559–569.

Woodruff DR, Meinzer FC, Lachenbruch B. 2008. Height-related trends in leaf xylem anatomy and shoot hydraulic characteristics in a tall conifer: safety versus efficiency in water transport. *New Phytologist* **180,** 90–99.

Yang SD, Tyree MT. 1993. Hydraulic resistance in *Acer saccharum* shoots and its influence on leaf water potential and transpiration. *Tree Physiology* **12,** 231–242.